UNIVERSIDAD NACIONAL DE COLOMBIA
SEDE MEDELLÍN
FACULTAD DE MINAS

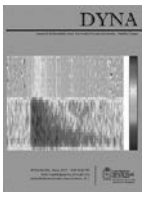

DYNA
http://dyna.medellin.unal.edu.co/

A shoreline-estimation system using remote radar sensing and image-processing techniques

Juan Carlos Vélez [a], Jhonathan Posada [b], Antonio Serrano [b], José Manjarrés [a], Juan Carlos Niebles [a] & Mauricio Pardo [a]

[a] *Electrical and Electronics Engineering Department, Universidad del Norte, Barranquilla, Colombia. jcvelez@uninorte.edu.co, jemanjarres@uninorte.edu.co, njuan@uninorte.edu.co, mpardo@uninorte.edu.co*
[b] *DST, Barranquilla, Colombia. antonio.r.smendoza@gmail.com, posadajhonatan@gmail.com*

Received: August 27th, 2015. Received in revised form: July 13th, 2016. Accepted: November 15th, 2016

Abstract
This paper proposes a radar-based sensing system that estimates the coordinates for shorelines based on image-processing techniques. The proposed system provides shore estimations without appreciable loss of resolution and avoids the costs associated with bathymetries and/or satellite images. The system is comprised of a commercial radar, a GPS, and a heading sensor, which communicates to a central node that georeferences the radar measurements and runs the image-processing algorithms. A dedicated FPGA-based unit is implemented to interface with the radar internal signaling to extract and deliver the radar information. In the central node, a novel mathematical model is proposed for georefencing radar measurements to WSG-84 coordinates. A seam-carving-like algorithm is applied over the estimated coordinates to create a shoreline based on a probability heat map. The system performance is validated using official geographical information, showing that a continuous shoreline can be generated with a CEP of up to 6 m without incurring elevated costs.

Keywords: mathematical coordinate mode; biased estimator; radar; FPGA-based system; kernel density estimation; heat map; seam carving.

Sistema para la estimación de orillas usando técnicas de sensado remoto con radar y procesamiento de imágenes

Resumen
Este trabajo propone un sistema de detección basado en radar para calcular las orillas de un rio usando procesamiento de imágenes. El sistema estima orillas sin pérdida apreciable en resolución evitando costos asociados con batimetrías y/o imágenes satelitales. El sistema está compuesto por un radar comercial, un GPS, y un sensor de rumbo que se comunican a un nodo central que georrefencia las mediciones del radar y ejecuta los algoritmos de procesamiento de imágenes. El hardware se basa en un FPGA para interactuar con la señalización interna del radar y extraer la información requerida. El nodo central implementa un novedoso modelo para georreferenciar las mediciones en coordenadas WSG-84. Posteriormente, un algoritmo de tipo "seam-carving" se aplica sobre las coordenadas estimadas para crear las orillas basándose en la probabilidad de la medición. El sistema se valida usando información oficial, y los resultados muestran un ECP de hasta 6 m.

Palabras clave: modelo matemático de coordenadas, estimador sesgado, radar, sistema a la medida implementado en FPGA, estimación basada en probabilidad, heat map, seam carving.

1. Introduction

Remote sensing applications have undergone major advancements based on the development of more efficient computational resources and RF technology. Tailored systems can be built with high acquisition rates at lower costs, facilitating the processing of larger amounts of information.

Commercial marine radars can be used to estimate surface patterns of water bodies and land entities [1,2]. However, the radars require intervention to obtain the complete clutter, which is usually not modified to display discrete targets.

Several systems that use radar-clutter have been reported. In [3], a sea-clutter retrieval and analysis was performed using a high-speed analog-to-digital converter (ADC) with a PCI interface to transfer and synchronize video signals. For example, the companies Miros and SeaDarQ offer sea-wave monitoring systems that can be

How to cite: Vélez, J. C., Posada, J., Serrano, A., Manjarrés, J., Niebles, J. C. & Pardo, M. A Shoreline-Estimation System using Remote Radar Sensing and Image-Processing Techniques DYNA 84 (200) 151-158, 2017.

used for oil-spill detection applications [4,5]. These systems have a similar hardware structure because they use standard radar outputs. The main inconvenience of this approach is the increased costs associated with robustness and wide-compatibility requirements, which are not necessary in every application.

In particular, this work considers the generation of navigation charts for rivers. The charts can be built using cartographic restitution via high-resolution radar/satellite images and high-precision GPS readings. This method offers charts with shoreline estimation with precision of approximately 1 m [6]. To achieve reliable results, it is necessary to apply techniques related to digital filtering on radar images available in the literature [7,8]. Some of the works employed image-processing techniques of rivers or beaches to estimate the corresponding shorelines; however, the system requires high-computational resources if the shorelines are to be updated continuously (i.e., as the vessel travels through the navigation path), and the cost of whole system (acquisition and processing) is still a concern [9, 10].

Another approach consists on the study of shorelines through high-resolution videos and RTK-GPS with accuracies of 1.1 m and 0.23 m, respectively [11]. In addition, the implementation of a Visual SLAM (Simultaneous Localization and Mapping) system has been considered [12]. Such a solution could be adapted to map river shorelines in real time by holding cameras on port, stern and bow. However, these systems have the disadvantage of video visibility and the associated limited detection range. The main justification for these methods and their expenses is the precision of the navigation charts. Thus, in the case of braided rivers, where the course changes frequently, the costs associated with the mentioned techniques cannot be afforded/justified because of the mandatory continuous chart updates.

Although the work reported in [2] used radar measurements, the novel approach is to employ the complete data, including the data that is discarded for the intended use of the radar, so that this whole clutter can be processed for the detection of river shores employing commercially marine radars. It is clear that well-known radar-image filtering techniques [7,8] cannot be directly used under this strategy. The system in [2] was complemented with a custom-made acquisition system that produced raw geographic information that properly transformed estimates the river coordinates. This prototype showed that it is possible to upgrade flexibility at reduced costs by sacrificing resolution compared to the use of bathymetries. The system must be optimized to achieve trade-off resolution, perform cluster definition, and minimize coordinate error with respect to the actual river shore. Safe navigation requires adequate signaling systems; in particular, for rivers with changing courses, traditional systems (e.g., buoys) are ineffective. As a result, alternative signaling strategies are required.

Thus, the motivation to propose cost-effective systems for navigation is two-fold. First, previous work [13,14] on river navigation assistance systems showed that shoreline mapping is possible, and further optimization is required to be considered as an effective navigation tool; and second, the Colombian government has indicated great interest in improving the use of sustainable fluvial transportation of cargo and passengers [15], as demonstrated by the large investments made recently. One of the most important challenges arises from the continuously changing nature of Colombian river courses and thus the changing nature of their navigable channels.

This paper discusses a system that uses commercial radars for effectively sensing shorelines. This work focuses on a more robust acquisition system and on alternative shoreline estimation using clutter optimization and an image-processing algorithm. First, both the hardware and the software of the system are described, and then the coordinate-transformation method that governs the acquisition and standardization of the sensed coordinates is presented. Next, the image-processing approach for generating continuous shorelines is described. Finally, the performance of the system is compared to official data to summarize system performance. Conclusions are drawn based on the performance evaluation.

2. Radar-Based system description

2.1. Hardware section

Marine radar systems usually have mechanically controlled rotating antennas. This implies that, besides the echo signals, additional signaling is required to determine antenna position and the beginning of the electromagnetic pulse, which leads to a composite output signal. The output video for most commercial marine radar systems is comprised of four signals: video, trigger, bearing and heading signals. The information obtained from marine radar systems is usually modified by means of filtering and thresholding stages, which avoid erroneous information and ease the interpretation of radar images [16].

A video signal consists of an electromagnetic echo shifted from the operating frequency to a baseband version. The video-signal amplitude at a defined time instant is closely related to the backscattered intensity reflected from a target area/volume in a given observation angle and range [6]. The presence of an echo in the video signal is determined by a trigger signal, which drives the modulated pulses transmitted by the antenna. The trigger signal defines the base time at which the received echo signal is synchronized.

The remaining signals are related to the mechanical operation of the antenna. The bearing signal is a highly steady signal that indicates the antenna angular position and is used by the radar as feedback for the antenna control stage. The signal period is inversely proportional to the antenna rotating speed. Finally, the heading signal indicates the beginning of an antenna turn allowing synchronization with the initial angle of the antenna rotation range.

Previous research has shown that echo signals received by radar antennas not only contain information from discrete targets but also from disperse ones, such as the sea, clouds, and terrain [17]. The complete information detected by the radar is called *clutter*. The clutter can be arranged as bi-dimensional arrays containing power spectral density information [17]; this information can be used to determine profiles that allow not only remote sensing but also shoreline estimation. Thus, the results of clutter analysis can be used for navigation chart generation and coastal erosion studies.

The devised system is based on a commercial radar system, Furuno M1715; the system is mounted in a vessel that scans a river. The vessel is equipped with both a GPS and a heading sensor that enable the geographical coordinates and the azimuthal angle (with respect to the geographical north) to be obtained in real time. The control unit that manages these components is comprised of a custom-made

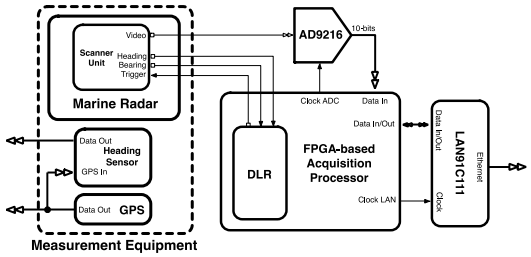

Figure 1. Block diagram of the proposed acquisition system.
Source: the authors.

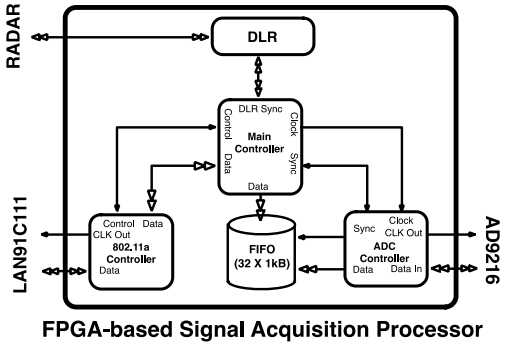

Figure 2. Block diagram of the proposed digital acquisition architecture.
Source: the authors.

Device-for-Link (DLR) module described using VHDL. The synchronization between the acquisition process and the transfer process is managed via radar display signaling (heading, bearing and trigger signals) by the DLR. The system is equipped with an AD9216 analog-to-digital converter that processes the video signal. This converter can handle conversion rates up to 105 Mbps [18]. In addition, the acquisition system contains an internal synchronous 1-K × 32-bit FIFO RAM that is implemented for buffering purposes. The data transfer to a main computer is managed by a LAN91C111 Ethernet controller, which supports a transfer rate up to 10 Mbps [19].

A hardware-described central core controls the different modules and performs the initial processing. All the VHDL modules are synthesized on an Altera Cyclone I FPGA EP1C20FC400. Fig. 1 shows the complete block diagram of the proposed acquisition system, and Fig. 2 shows the components of the FGPA-based central core.

2.1.1. Device-for-Link (DLR), ADC controller hardware modules

The DLR and ADC controller work together to receive the clutter. The DLR synchronizes with the radar antenna through the composite radar signaling using the heading, bearing and trigger signals.

The ADC Controller Driver controls the detection and conversion of the radar composite video signals. This driver also scales down the input clock to establish a 25 MHz ADC sample frequency, which allows a signal resolution of approximately 12 m.

To gather the clutter, the DLR and ADC Controller work together, and the synchronization of both modules is performed by the Main Controller. First, the DLR waits for the start of an antenna turn by monitoring the heading signal. Next, the DLR monitors the trigger signal to inform the Main Controller to command the ADC Controller to acquire a number of samples related to the desired range resolution. The bearing signal is used to estimate the current angular position of the antenna to overcome Pulse Repetition Frequency (PRF) variations caused by external forces. The ADC Controller receives 10-bit words obtained from the radar measurements, and conforms 32-bit words that include the status of the bearing signal.

To facilitate the packet assembly for transfer to the computer, the amount of measurements acquired per trigger pulse is a multiple of three, which also optimizes data transfer. The system supports clutter acquisition at two maximum possible ranges: 0.75 nmi and 1.5 nmi.

2.1.2. Memory module

Each 32-bit word is temporally stored in the internal buffer for later transfer to the external LAN controller. The RAM memory is designed such that it takes advantage of both falling and rising edges of the clock signal for input/output operations. In a falling edge, the embedded RAM address register is loaded/retrieved with the proper value. Next, in the next rising edge, the address register is incremented/decremented as required, depending on the operation.

The FIFO-memory control lines are shared by two internal cores: the Main Controller, which has the ability to execute read operations (POP), and the ADC controller, which has the ability to execute write operations (PUSH). This scheme allows real-time clutter acquisition and proper buffering for later transfer.

2.1.3. Ethernet controller driver hardware module

The Ethernet Controller Driver handles the physical layer of the communication to a computer by controlling the operation of the LAN91C111. The data transfer is achieved using the User Datagram Protocol (UDP) as broadcast packets. The communication flow is specifically designed for point-to-point transfer (with no intermediate routers or hubs) to optimize the link usage. The packet size varies, depending on the desired range.

This structure is defined to reduce the overhead while guaranteeing proper signal reconstruction by maintaining a number identifier through an antenna-turn indicator. The maximum number of echo signals that fit in a single UDP packet depends on the acquired range; however, the data packet limit is 1,500 bytes.

The designed driver has the ability to read and write the registers of the LAN91C111 controller and incorporates setup routines, which relieves the Main Controller from executing them. The driver signaling is designed to operate using 4-bit commands, which includes the following actions:

Link Configuration (0x0): Establishes the link speed and activates the physical layer on the LAN91C111 controller. As a result, the computer is set to receive data from the acquisition system.

Memory Allocation (0x1): Executes an internal operation on the LAN91C111 controller, which frees space on the controller internal FIFO memory, allowing the insertion of the UDP packets to transmit.

FIFO Writing (0x2): Writes the radar-signal data to the LAN91C111 internal FIFO memory.

Start Transmission (0x3): Starts the UDP packet transfer from the LAN91C111 controller to the main computer.
Set Header (0x4): Establishes the packet identifier number.

2.2. Software section

The software component of this system is completely custom-made. A specific software program is created for interfacing the radar and obtaining the clutter. Next, the whole radar measurement processing is performed using MATLAB. This platform eases the mathematical implementation of the model described in Section 3.2.

The main computer runs algorithms that segment, georeference, and estimate the river shores using the WGS84 standard. In addition, the computer reconstructs the image from the radar and attaches the coordinates and azimuth angles from the GPS and heading sensor, thereby ensuring the system gathers all the information in the same frame. The process of acquiring the radar image controls when the complete system must operate.

Because the hardware sends UDP packets in a very specific format, a custom application is required for receiving and interpreting the data properly in the host computer. The main functions of the related application software are:

- Setting up an UDP port socket in the host computer.
- Listening continuously the port for UDP packets.
- Synchronizing the downloading process of the acquired radar samples.
- Visualizing radar images in real time extracted from the UDP packets with the corresponding azimuth angle.
- Storing the acquired radar samples in files of convenient raw format.
- Accessing previously stored radar images for user review.
- Configuring and managing the application that can generate files exportable to Google Earth.

3. Mathematical model for coordinate estimation

3.1. Pre-processing of radar images

Clutter obtained from the proposed acquisition system is in polar coordinates disposed in a rectangular grid, known as the B-scope format. The B-scope format represents the bearing and distance from the radar and therefore is not suitable for shoreline coordinate estimation. Thus, a spatial translation using interpolation operations is required to prepare data for processing and analysis. The basic theory on radar-signal scan conversion can be found in [20].

The conversion of a radar data array from a B-scope format to a Cartesian one is accomplished using an interpolation kernel to estimate the intensity values of the B-scope data array into the coordinates corresponding to the Cartesian system. The kernel size is related to the interpolation accuracy. This work implements a bi-cubic interpolation kernel, as proposed in [21]. The equation that summarizes the scan conversion operation is:

$$I(\rho,\theta) = \sum_l \sum_m B_{lm} u\big(f(\rho)\big)\, u\big(g(\theta)\big), \quad (1)$$

where $I(\rho,\theta)$ is the interpolated matrix, and (ρ,θ) are the polar coordinates that are to be converted into the Cartesian domain. The term B_{lm} corresponds to a given position within the B-scope formatted matrix, and $u(\cdot)$ is the interpolation kernel.

3.2. Mathematical model

It is necessary to develop a mathematical model to georeference shorelines from rivers. Such a model must calculate the coordinates of distant objects using data given by the radar and transforming the spatial reference into a geocentric reference. Fig. 3a shows an example situation of obtaining coordinates for a shoreline point. Here, let θ be the azimuth given by the electronic compass, R the distance from radar, λ_{GPS} and ϕ_{GPS} the WGS84 coordinates from a GPS. Fig. 3b presents the Cartesian projection of the position and the orientation of a ship corrected by the θ angle, such that it points to the geographical north [20].

To obtain the local rectangular reference on Fig. 3b, the position of any object can be described with a north-direction projection labeled *dN* and defined as $Rcos(\theta+\alpha)$ along with an east-direction projection *dE* equal to $Rsin(\theta+\alpha)$. However, this local reference must be mapped to the standard.

A solution is presented in [22] using transformations from [17] to convert from plane coordinates to ellipsoidal for the different datum of Colombia. However, that model requires data closely related with each geographical zone and consequently represents a limitation for navigation on rivers that have not been studied or cover a large land area. Thus, for a universal Cartesian projection, a transformation function must be defined for every point on the terrestrial ellipsoid. Thus, the ship and the near shorelines are assumed to be in the same tangent plane because there are no significant changes on the ellipsoidal height. Geocentric Cartesian coordinates for a shoreline point (x, y, z) are then defined as a function of displacements from the ship coordinates $(xGPS, yGPS, zGPS)$ as:

$$[\Delta x, \Delta y, \Delta z] = [x - x_{GPS}, y - y_{GPS}, z - z_{GPS}]. \quad (2)$$

The objective is to find unit vectors to direct displacements *dN* and *dE* and transform them to the form (2). According to [20], the rectangular coordinates for GPS can be obtained from a function of ellipsoidal parameters as

$$\vec{r}(\lambda,\phi,h) = x\hat{\imath} + y\hat{\jmath} + z\hat{k} = (\eta(\phi)+h)\cos(\phi)\cos(\lambda)\,\hat{\imath} + (\eta(\phi)+h)\cos(\phi)\sin(\lambda)\,\hat{\jmath} + \big((1-e^2)\eta(\phi)+h\big)\sin(\phi)\,\hat{k}\ , \quad (3)$$

$$\eta = \frac{a}{\sqrt{1-e^2\sin^2\phi}}, \quad (4)$$

where e^2 is the first eccentricity of ellipsoid, and a is the minor semi-axis parameter of the WGS84 standard. Notice that $\vec{r}(\lambda)\big|_{(\phi_{GPS},h_{GPS})}$ and $\vec{r}(\phi)\big|_{(\lambda_{GPS},h_{GPS})}$ describe a parallel and a meridian passing through $(\lambda_{GPS}, \phi_{GPS}, h_{GPS})$, respectively. Thus, unit vectors for the north and west directions can be obtained as follows:

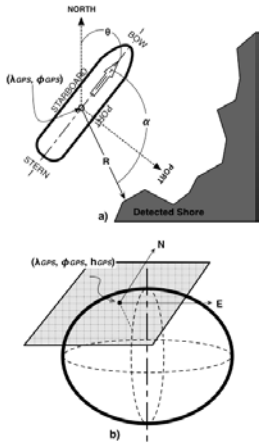

Figure 3. Illustration of the geometric considerations for the mathematical model. Source: the authors.

$$\vec{N}(\lambda,\phi,h)=\frac{\frac{\partial\vec{r}}{\partial\phi}}{\left|\frac{\partial\vec{r}}{\partial\phi}\right|}$$

$$=\begin{bmatrix}-\sin(\lambda)\cos(\phi)\left[\dfrac{a}{(1-e^2\sin^2\phi)^{\frac{1}{2}}}+h\right]\hat{\imath}\\ \cos(\lambda)\cos(\phi)\left[\dfrac{a}{(1-e^2\sin^2\phi)^{\frac{1}{2}}}+h\right]\hat{\jmath}\end{bmatrix} \quad (5)$$

$$\vec{E}(\lambda,\phi,h)=\frac{\frac{\partial\vec{r}}{\partial\phi}}{\left|\frac{\partial\vec{r}}{\partial\phi}\right|}=$$

$$\begin{bmatrix}-\sin(\lambda)\cos(\phi)\left[\frac{a}{\sqrt{e_2}}+h\right]\hat{\imath}\\ \cos(\lambda)\cos(\phi)\left[\frac{a}{\sqrt{e_2}}+h\right]\hat{\jmath}\end{bmatrix} \quad (6)$$

Both k components are zero because there is no height variation. Finally, the coordinates for a shoreline point can be defined as

$$\begin{bmatrix}x\\ y\\ z\end{bmatrix}=\begin{bmatrix}x_{GPS}\\ y_{GPS}\\ z_{GPS}\end{bmatrix}+d_N\vec{N}(\lambda_{GPS},\phi_{GPS},h_{GPS})+d_E\vec{E}(\lambda_{GPS},\phi_{GPS},h_{GPS}). \quad (7)$$

Eq. (7) describes a mathematical model that takes θ, R, λ_{GPS}, ϕ_{GPS}, and returns rectangular coordinates of a shoreline point. Finally, for coordinates using the WGS84 standard, the following transformation must be applied:

$$\vartheta=\arctan\left(\frac{z_p a}{\sqrt{x_p^2+y_p^2 b}}\right) \quad (8)$$

$$\begin{bmatrix}\lambda_p\\ \phi_p\\ h_p\end{bmatrix}=\begin{bmatrix}\arctan\left(\dfrac{y_p}{x_p}\right)\\ \arctan\left(\dfrac{z_p e^2 b\sin^3\vartheta}{\sqrt{x_p^2+y_p^2}-e^2 a\cos^3\vartheta}\right)\\ \dfrac{\sqrt{x_p^2+y_p^2}}{\cos\phi}-\dfrac{a}{\sqrt{1-e^2\sin^2\phi}}\end{bmatrix}. \quad (9)$$

3.3. Shoreline coordinate estimation

Even though the mathematical model for georeferencing is deterministic, the output from the acquisition system (transformation step) is a series of data that deviates from the actual desired coordinate because of random errors from the GPS, radar and the heading sensor. In addition, there are multiple detections that the radar can generate of the same shore sector. Thus, when all these coordinates are superposed, the river shore takes the form of a scattered object that contains several estimations of the sector. Fig. 4 shows the visualization of a sample of transformed coordinates from the radar on top of a Google Earth image.

The sector is located in the Madgalena River base level (Barranquilla, Colombia). As observed, there are several points for the same sector; therefore, a method is required to consolidate measurements into a single coordinate that characterizes the shore sector. The concept is analogous to the reception of data points in a digital communication system, and the estimation of the actual point is made using a signal-space diagram.

To avoid resolution constraints due to clustering techniques [2], the problem of shoreline estimation is treated as an image-processing problem. To that end, the coordinate measurements are assumed as a random variable that is distributed according to a density function (pdf) that has high probability closer to shore locations and low probability further from the shore. The goal is to estimate this pdf using kernel density estimation (KDE) [23]. Thus, each measured coordinate is associated with a 2D local Gaussian distribution, with the mean equal to the measured coordinate and the variance proportional to the radar resolution.

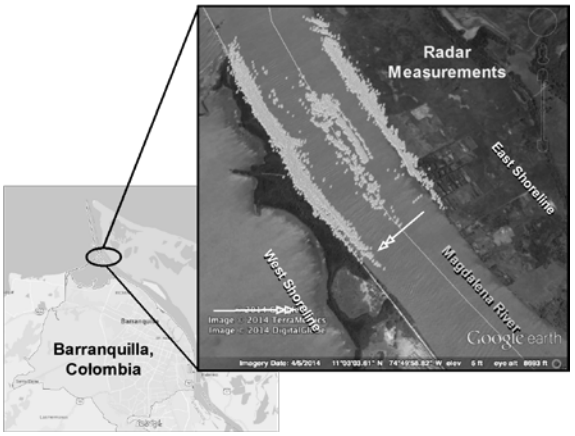

Figure 4. Raw measured data processed by the acquisition system. Output of the coordinate transformation stage.
Source: the authors.

Once the shore pdf is estimated, the range of the resultant density function is color coded to conform to a heat map of the coordinates. The color is related to the probability of the location of the shore at a given coordinate.

Last, a seam-carving-like algorithm [24] is applied to the heat map, with the goal of generating a single path that resembles the shoreline. The algorithm generates the shortest path that traverses the heat map by visiting contiguous coordinates with maximum probability. The optimum path will become the estimated shoreline.

4. Shore estimation test and results

The base level of the Magdalena River was selected for testing. Even though the shores at this point are relatively constant, a complete set of very accurate coordinates is available for comparison; therefore, the test will show if the complete estimation strategy produces adequate results. The information for shores is provided by Instituto de Estudios Hidráulicos y Ambientales (IDEHA) of Universidad del Norte, which conducts regularly scheduled bathymetries for the operation of the fluvial port of Barranquilla, Colombia [25]. IDEHA maintains both historic and updated data of the area.

First, the Furuno M1715 radar is located at a fixed point in the river, and the measurement is made. The acquisition system receives the echoes from the radar, and the relative distance from the radar is transformed into WSG84 coordinates using GPS and heading sensor (Section IIIB). Because the acquisition system captures and reconstructs the image from the clutter, the relationship between the coordinate (distance) and the pixel is obtained. The settings of the Furuno M1715 radar produce 140 pixels per 278 m. This relationship is important because the next step in the process is to translate the transformed coordinates into pixels to generate the necessary images for shore estimation. Fig. 5 shows a larger measurement area compared to Fig. 4 but using pixels as the measuring unit.

Next, a 2D Gaussian distribution is attached to each point of the cloud, as shown in Fig. 5. The sigma of the Gaussian is selected to connect as many close points as possible while keeping the estimation error to a minimum. As expected, only at the end of the process can the selected sigma be adjusted to produce a better shoreline estimation. This value can be reduced if the radar sweeps the target sector several times and/or the speed of the vessel that carries the radar is kept slow (for this work, the radar swept a target sector once traveling at 10 KPH).

After applying KDE, the probability density will be higher when more measurements of a point are aggregated. A heat map can therefore be generated that displays regions with increased confidence of the measurement. The heat map corresponding to the selected river section is shown in Fig. 6 (using a sigma equal to 2.5 pixels). From Fig. 6, it can be concluded that the "red regions" are those where the confidence of the measurement is higher, and hence the probability that the actual shore passes through those should be higher. To avoid clustering the images creating areas of decision, the goal of this work is to propose a method to generate a continuous shoreline that, in effect, provides full resolution. Thus, the idea is to connect those points of higher confidence while the line length within the image is kept to a minimum.

The technique is inspired by the Seam Carving algorithm for content-aware image resizing [24]. This algorithm establishes a number of seams (paths of least importance) in an image that allows reduction of an image by removing seams or extension of an image by inserting seams. By definition, a seam is either vertical or horizontal. In any case, an importance/energy function is evaluated per pixel by measuring its contrast with its neighbor pixels. Generating a seam consists of finding the path of minimum energy cost from one end of the image to the other.

Thus, the seam concept can be applied to Fig. 6 if the image is rotated and the heat map inverted. Image rotation is required to "align" the more confident sections either vertically or horizontally, and inverting the heat map will transform the "red points" to valleys or points with less energy. Using matrix-based math software, such as iPython, rotation and inversion are handled as matrices facilitating the inverse operations. Fig. 7 shows the two seams (one per shore) once the image is returned to its initial position.

Finally, to evaluate the estimation using the seams, a set of official coordinates provided by IDEHA are transferred to Fig. 7 using the already defined coordinate-pixel transformation. Given the size of the image in pixels (900 × 1000), it can be concluded that the estimation using seams is adequate only by visual inspection.

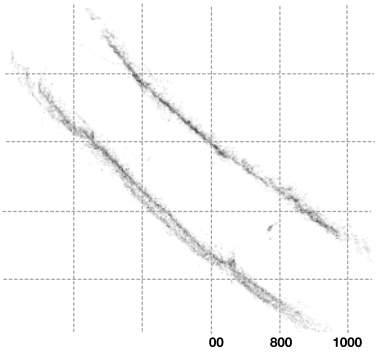

Figure 5. Detected coordinates transformed to pixels. A degrees-pixel transformation is generated.
Source: the authors.

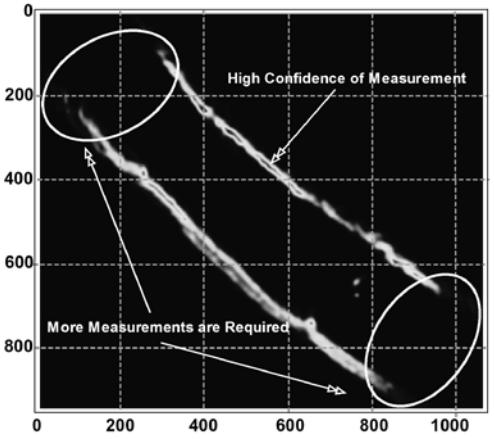

Figure 6. Heat map generated from the KDE of the measurement coordinates.
Source: the authors.

To generate error measurements, the image is analyzed to generate the minimum distance (in pixels) from the seam to an IDEHA coordinate. Thus, the IDEHA coordinates are mapped into pixels by means of a matrix transformation. Because the IDEHA coordinates are a finite set of numbers, a histogram is generated using pixels (distance) as variables (Fig. 8). The use of iPython enables the use of the Python Data Analysis Library, better known as *pandas*. As described in its website, *pandas* is an open source, BSD-licensed library providing high-performance, easy-to-use data structures and data analysis tools for the Python programming language [26]. *Pandas* reports that most of the distances are grouped in the 0 to 4 pixel range, which validates the image-processing approach for shore estimation. Among other measurements (Table 1), the minimum distance obtained in this exercise corresponds to 1 pixel (1.98 m), whereas the maximum is equal to 11 pixels (22.2 m). However, for this system, the most suitable performance measurement corresponds to the Circular Error Probable (CEP). The CEP is a measure of the system precision and can be defined as the radius of a circle, centered about the mean, whose boundary is expected to include 50% of the radar measurement for a given coordinate. For the image-processing approach, *pandas* reports an ECP of approximately 6 m. Table 1 summarizes additional error measurements of the proposed system with respect to the officially accepted shoreline coordinates provided by IDEHA.

Finally, the seams are transformed into coordinates and plotted along the IDEHA points in a georeferenced image, such as Google Earth, to visually observe the result of the process (Fig. 9).

5. Conclusions

This paper presented a radar-based sensing system to estimate the coordinates for river shores. The proposed system is complemented with image-processing algorithms to generate continuous shorelines while avoiding resolution errors from clustering techniques. The proposed technique was shown to be technically viable and able to reduce the costs for updating navigation charts.

A mathematical model based on the projection of parametric curves describing the planet as an ellipsoid allows its use without any geographical restriction. Next, once the coordinates are expressed in the WSG84 standard, they are transferred to a 2D grid as image pixels. This translation allows handling the estimation task as an image-processing problem. The idea is to generate a continuous line that describes the desired shoreline. The system was validated in an actual environment using the data provided by IDEHA, which maintains accurate historic and updated shore coordinates for the base level of the Magdalena River. Based on the validation results, the system was found to perform with a resolution of approximately 1.98 m, which is equivalent to 1 pixel, and a Circular Error Probable (CEP) of 6.28 m.

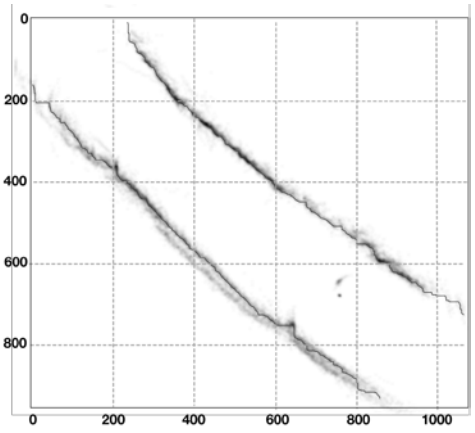

Figure 7. Shorelines as a result of the seam-carving algorithm.
Source: the authors

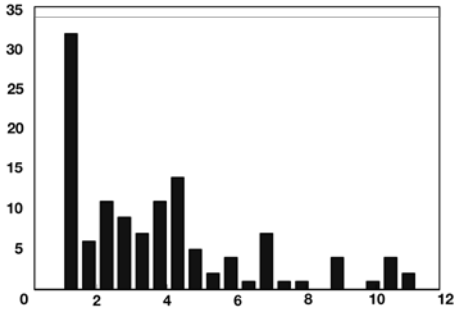

Figure 8. Histogram in pixels of the estimated shoreline error with respect to the IDEHA coordinates.
Source: the authors

Table 1.
Final Error Measurement Comparison

System	MAX [m]	MIN [m]	STD [m]	CEP [m]	RMS [m]	Resolution [m]
This work	22.2	1.98	5.28	6.28	8.19	1.98

Source: the authors

Figure 9. Comparison of the shore coordinates between the radar-based system and the data from IDEHA using a georreferenced image.
Source: the authors

The use of the image-processing technique showed that the problem of shoreline estimation can be improved as more radar measurements of a defined sector are available. More measurements of a sector translate into a higher probability in the heat map and therefore force the seam to connect in that sector. Sweeping the radar several times and/or reducing the speed at which the radar moves in the vessel can achieve the goal of increasing the number of measurements. Improving the cloud of points (Fig. 6) allows reducing the sigma of each Gaussian distribution associated with a point, thereby reducing the wandering of a seam and reducing errors.

It is possible to improve the statistics with more accurate equipment; however, local cargo companies have accepted these indicators. The costs of the proposed technique are far more convenient than the use of satellite photos and/or bathymetries; however, to guarantee the output of the shoreline estimation mechanism, an initial costly method can be employed, so that error

measurements can be defined, which later allows affordable navigation chart updating process using the proposed method.

References

[1] Alpers, W., Ross, D. and Rufenach, C., On the detectability of ocean waves by real and synthetic aperture radar, Journal of Geophysical Research, 86, pp. 6481-6498, July, 1981. DOI: 10.1029/JC086iC07p06481

[2] Posada, J., Pardo, M., Velez, J.C. and Alvarado, M., Radar-based georeferencing system for estimation of changing river-shores, IEEE International Symposium on Circuits and Systems (ISCAS), pp.2495-2498, 2014. DOI: 10.1109/ISCAS.2014.6865679

[3] Reichert, K., Hessner, K., Nieto, J.C. and Dittmer, J., Wamos II: A radar based wave and current monitoring system, ISOPE '99, Brest, Proceedings, 3, May, pp. 1-5, 1999.

[4] Miros, A.S., Wavex monitoring system datasheet. [online]. Available: http://www.miros.no.

[5] Nortek, B.V., SeaDarQ oil detection with radar. [online]. Available: http://www.seadarq.com.

[6] Cracknell, A. and Hayes, L., Introduction to remote sensing, Taylor & Francis, 2 ed., pp. 21-71, 2007.

[7] Frost, V., Stiles, J., Shanmugan, K. and Holtzman, J.C., A model for radar images and its application to adaptive digital filtering of multiplicative noise. IEEE Transactions on Pattern Analysis and Machine Intelligence, PAMI-4(2), pp. 157-166, 1982. DOI: 10.1109/TPAMI.1982.4767223

[8] Lillesand, T., Kiefer, W. and Chipman, J., Remote Sensing and Imafe Interpretation, 6th edition. Wiley, 2007.

[9] Louati, M., Saïdi, H. and Zargouni, F., Shoreline change assessment using remote sensing and GIS techniques: a case study of the Medjerda delta coast, Tunisia. Arabian Journal of Geosciences, 8(6), pp. 4239-4255, 2015. DOI: 10.1007/s12517-014-1472-1

[10] Lipakis, M., Chrysoulakis, N. and Kamarianakis, Y., Shoreline extraction using satellite imagery. In: Pranzini, E. and Wetzel, E. (eds): Beach erosion monitoring. Results from BEACHMED/e-OpTIMAL Project (Optimization des techniques integrées de monitorage appliquées aux Lottoraux) INTERREG IIIC South. Nuova Grafica Fiorentina, Florence, Italy, pp. 81-95, 2008.

[11] Harley, M., et. al., Assessment and integration of conventional, RTK-GPS and image-derived beach survey methods for daily to decadal coastal monitoring, Coastal Engineering Journal, 2010. DOI: 10.1016/j.coastaleng.2010.09.006

[12] Díaz, A., Paz, L., Caicedo, E. and Piniés, P., Simultaneous localization of a monocular camera and mapping of the environment in real time, DYNA, [online]. 81(183), pp. 7-15, 2014. Available at: http://www.redalyc.org/articulo.oa?id=49630072002

[13] Flórez, D., Posada, J., Devia, C., Reyes, L., Vélez, J.C. y Alvarado, M., Actualización del sistema satelital de asistencia a la navegación. XX Seminario Nacional de Hidráulica e Hidrología, Barranquilla, Colombia, Agosto, 2012.

[14] Vélez, J.C., y Alvarado, M., Sistema satelital de asistencia a la navegación fluvial – SNS, Revista de Ingeniería, Sociedad de Ingenieros, 928, pp. 76-79, 2013.

[15] Col. DNP. Visión Colombia II Centenario: Generar una infraestructura adecuada para el desarrollo. Bogotá DC: Dirección Nacional de Planeación, 2004.

[16] Sanyo Electric, LC79401D Dot-Matrix LCD Driver Datasheet, 1995.

[17] Torge, W., Geodesy, De Gruyter, 3rd Edition, 416 P., Berlín, 2001.

[18] Analog Devices Inc., AD9216 Dual A/D Converter Datasheet Rev. A, 2005.

[19] SMSC, LAN91C111 10/100 Non-PCI Ethernet Single Chip Rev. C, 2011.

[20] Nickerson, K. and Haykin, S., Scan conversion of radar images, IEEE Transactions on Aerospace and Electronic Systems I, 25, pp. 166-175, 1989. DOI: 10.1109/7.18678

[21] Keys, R., Cubic convolution interpolation for digital image processing, IEEE Transactions on Acoustics, 29, pp. 1153-1160, 1981. DOI: 10.1109/TASSP.1981.1163711.

[22] Col. IGAC. Adopción del marco geocéntrico nacional de referencia MAGNA-SIRGAS como datum oficial de Colombia. Bogotá DC: Instituto Geográfico Agustín Codazzi, 2004.

[23] Duong, T., An introduction to kernel density estimation, University of Western Australia, Australia, 2001.

[24] Avidan, S., y Shamir, A., Seam carving for content-aware image resizing, ACM Trans. on Graphics, 26(3), 2007. DOI: 10.1145/1276377.1276390

[25] Alvarado, M., et. al., Rio Magdalena: Navegación marítima y fluvial (1986 - 2008), Ediciones Uninorte, Barranquilla, 2008.

[26] Lambda Foundry and PyData Development Team. Python Data Analysis Library, [online]. 2011. [Consulted September 15, 2014]. Available at: http://pandas.pydata.org/

J.C. Vélez, received BSc. and MSc degrees in Telecommunications Engineering from the Ukranian State Academy of Telecommunications (USAT) in 1995, and the PhD. degree in Radioelectronics from the Moscow Power Institute (TU)-MPEI in 2004. In July 2004, he joined the faculty of Universidad del Norte, Barranquilla, Colombia, where he is an associate professor in the Department of Electrical and Electronics Engineering. In 2008, he was a visiting scholar in the National University of Colombia, where he worked as a researcher in radar and telecommunications. His research interests are in the areas of radio engineering, radio navigation, radars and TV Systems. Dr. Velez's achievements include a scholarship for undergraduate studies from the Soviet Union in 1989, a Diploma of Engineering (honors) from the USAT in 1995, and a Diploma for Best Presentation in the 9th and 10th International Conferences on Radio Electronics, Electrical and Electronics Engineering in 2003 and 2004, respectively.
ORCID: 0000-0002-3953-6297

J. Posada, received BSc. and MSc. degrees in Electronics Engineering from Universidad del Norte, Barranquilla, Colombia, in 2008 and 2011, respectively. Mr. Posada worked as a teaching assistant during his graduate studies and also as a research engineer in projects related to navigation on Colombian rivers. Mr. Posada has created nautical data generator software that has evolved into one of the software standards for Colombia. Mr. Posada currently works in the industry since 2012 as an Innovation and Technology Engineer.
ORCID: 0000-0001-7025-9067

A. Serrano, received BSc. and MSc. degrees in Electronics Engineering from Universidad del Norte, Barranquilla, Colombia, in 2010 and 2012, respectively. Mr. Serrano graduated with honors in both the BSc. and MSc. programs. Mr. Serrano worked as a junior research from 2010 and 2012 and as a Research Scientist from 2012 to 2013. Mr. Serrano currently works in industry (since 2013) as a Product Engineer in DST LTDA.
ORCID: 0000-0003-0500-5786

J. Manjarrés, received a BSc. degree in Electronics Engineering and a BSc. degree in Mathematics from Universidad del Norte, Barranquilla, Colombia in 2014 and 2015, respectively. Mr. Manjarrés is working as a Teaching Assistant and Research Assistant at Universidad del Norte, as he begins his graduate studies in this institution.
ORCID: 0000-0003-0532-9449

J.C. Niebles, received a BSc. degree in Electronics Engineering from Universidad del Norte, Barranquilla, Colombia, in 2002, a MSc. degree in Electrical and Computer Engineering from the University of Illinois at Urbana-Champaign in 2007, and a PhD. degree in Electrical Engineering from Princeton University in 2011. Currently, he is a senior research Scientist in the Computer Science Department at Stanford University (since 2015), and also an assistant professor in Electrical and Electronic Engineering in Universidad del Norte (Barranquilla, Colombia), since 2011. His computer vision research is sponsored by a Google Faculty Research award (2015), the Microsoft Research Faculty Fellowship (2012), a Google Research award (2011) and the Colombian science agency – COLCIENCIAS (2011, 2014).
ORCID: 0000-0001-8225-9793

Mauricio Pardo received a BSc. degree in Electronics Engineering from Universidad del Norte, Barranquilla, Colombia, in 2002, and MSc. and PhD. degrees in electrical engineering from the Georgia Institute of Technology, Atlanta, GA, in 2007 and 2012, respectively. In January 2003, he joined the faculty of Universidad del Norte, Barranquilla, Colombia as an instructor in the Department of Electrical and Electronics Engineering. In August 2004, he was the Undergraduate Program Coordinator at the same university. Dr. Pardo is currently the Electronics and Electrical Engineering Department Chair and leads the electronic analog design area. His research interests are in the areas of oscillators and PLLs for clock cleaners and frequency synthesizers. Mr. Pardo was a 2005 recipient of the Fulbright/Colciencias/DNP Scholarship to pursue his doctoral studies in electronic design applications and microelectronics. Mr. Pardo serves as President of the IEEE Colombian Caribbean Subsection from 2013.
ORCID: 0000-0002-7608-3290